

Probing cold nuclear matter effects with the productions of isolated- γ and γ +jet in p+Pb collisions at $\sqrt{s_{NN}} = 8.16$ TeV

Guo-Yang Ma,¹ Wei Dai*,² and Ben-Wei Zhang^{†1}

¹Key Laboratory of Quark & Lepton Physics (MOE) and Institute of Particle Physics, Central China Normal University, Wuhan 430079, China

²School of Mathematics and Physics, China University of Geosciences, Wuhan 430079, China

(Dated: January 11, 2019)

We investigate the cold nuclear matter (CNM) effects on the productions of the isolated prompt photon and γ +jet in proton-lead collisions at 8.16 TeV under the next-to-leading order (NLO) perturbative quantum chromodynamics calculations with four parametrizations for nuclear parton distribution functions (nPDFs), *i.e.* DSSZ, EPPS16, nCTEQ15, nIMPArton. Our theoretical calculations provide good descriptions of pp baseline in the ATLAS collaboration and make predictions for future experimental results at p+Pb collisions. We calculate the dependence of the nuclear modification factor of isolated prompt photon on transverse momentum p_T^γ and pseudo-rapidity η^γ at very forward and backward rapidity regions, and demonstrate that the forward-to-backward yield asymmetries Y_{pPb}^{asym} as a function of p_T^γ with different nPDFs parametrizations have diverse behaviors. Furthermore, the nuclear modification factor of isolated- γ +jet $R_{pPb}^{\gamma\text{Jet}}$ as a function of γ +jet's pseudo-rapidity $\eta_{\gamma\text{Jet}} = \frac{1}{2}(\eta_\gamma + \eta_{\text{Jet}})$ at different average transverse momentum $p_T^{\text{avg}} = \frac{1}{2}(p_T^\gamma + p_T^{\text{Jet}})$ has been discussed, which can facilitate a tomography study of CNM effects with precise locations in a rather wide kinematic region by varying the transverse momenta and rapidities of both isolated photon and jet in p+A collisions.

PACS numbers: 12.38.Mh; 25.75.-q; 13.85.Ni

1 INTRODUCTION

In high energy nuclear physics, productions of prompt photon and photon associated jet with high transverse momentum are valuable observations of the short-distance dynamics of quarks and gluons [1]. Since prompt photon is precisely calculable by perturbative quantum chromodynamics (pQCD) at higher order corrections and carries no color charge like other gauge bosons, it has been widely regarded as an optimal probe of the initial state of the collisions[2–6], as well as an excellent tag of inersive parton (jet) to quantify the mechanisms of jet quenching in ultra-relativistic heavy ion collisions [7–14]. In the past few years, ATLAS [15–17] and CMS [18–20] collaborations have made lots of measurements on isolated prompt photon and γ +jet productions in proton-proton, proton-nucleus and nucleus-nucleus collisions. The isolated photon's nuclear modification factor depending on photon transverse energy E_T^γ measured in most central PbPb collisions has large uncertainty, it also shows centrality dependence at limited E_T^γ intervals [7]. And γ +jet events have been discussed to extend the study on the tomography of quark-gluon plasma(QGP) created in heavy ion collisions. For instance, the distribution of photon plus jet transverse momentum imbalance ($x_{j\gamma} = p_T^{\text{jet}}/p_T^\gamma$) indicates that a larger part of jet's initial

energy would be damped and deposited in most central Pb+Pb collisions[20]. In this study we may employ the productions of isolated photon and photon+jet in p+A collisions to probe the initial-state cold nuclear matter (CNM) effects.

In elementary hadron-hadron collisions, with the perturbative QCD (pQCD), the cross section of leading particle (and jet) in general could be expressed as an convolution of the parton distribution functions (PDFs), and the hard partonic cross section, and the fragmentation functions (FFs) if applicable. The parton distribution function (PDF) for a parton i from the free proton ($f_i^p(x, Q^2)$) is of nonperturbative property in the frame of the QCD collinear factorization theorem [21, 22] and its evolution in the scale Q^2 can be depicted as the DGLAP equations [23–25]. In p+A collisions, PDFs in nuclear environment should be modified due to different CNM effects, such as shadowing, anti-shadowing, EMC effect and Fermi motion *etc.* [26]. It is expected that the QCD factorization theorem may hold for nuclei as a good approximation, and we can replace the PDF in a free proton ($f_i^p(x, Q^2)$) with the nuclear PDF ($f_i^A(x, Q^2)$) to effectively include different CNM effects to study hard processes in p+A collisions.

In past three decades, our understanding on the global fits of nuclear PDFs (nPDFs) have been regularly enriched by the growing experimental results of the fixed-target deeply inelastic scattering (DIS) and low-mass Drell-Yan (DY) dilepton measurements [27–29] and the theoretical predictions from leading order (LO) up to next-to-next-to-leading order (NNLO) [30–33]. In the

*weidai@cug.edu.cn

†bwzhang@mail.cnu.edu.cn

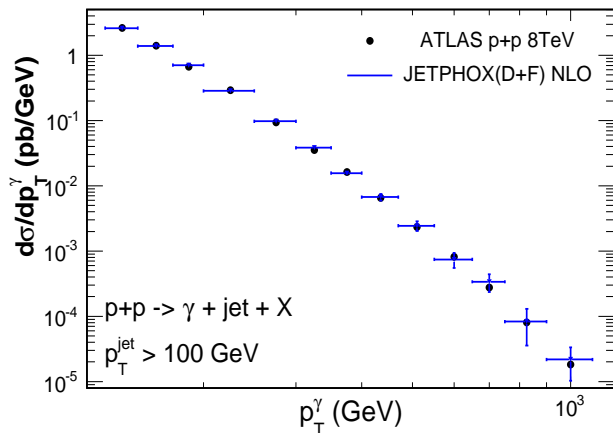


FIG. 1: The cross section of isolated photon plus jet as function of p_T^γ in p + p collisions at 8 TeV and the NLO pQCD theoretical calculations(JETHOX).

DSSZ framework [34], the global analysis for the nPDFs is presented as the ratio of parton distributions in a proton of a nucleus and in the free proton, $R_i^A(x, Q^2) = f_i^A(x, Q^2)/f_i^p(x, Q^2)$ evolving at initial scale $Q_0 = 1$ GeV. The DSSZ analysis not only uses the l^\pm/μ -DIS data sets and p+A DY data sets, but also firstly includes the inclusive pion production in the deuteron and gold collisions at PHENIX to constrain the nuclear gluon PDF. The EPPS16 [35] is the extension of the previous EPS09 [36] with the additional experimental data from proton-lead collisions at LHC [37–39] for the first time. It offers a less biased and flavor-dependent fitting analysis for nuclear PDFs. Following the CTEQ global PDF fitting framework [31, 40, 41], nCTEQ15 [42] describes the nuclear dependence of nPDFs at NLO on different nuclei, including Pb. The nIMParton [43] is a global analysis based on two data sets of nuclear DIS data, which either only contains isospin-scalar nuclei or all nuclear data. The difference of the fitting functions obtained by these two data sets is on the shadowing (small x region) effects. In addition, the Fermi motion and off-shell effect, nucleon swelling, and parton-parton recombination are taken into account together in the nIMParton framework. In the market, some other parameterizations of nPDFs have also been proposed [44–48], and so far due to the lack of enough experimental data, limited constraints and large uncertainties appear in nuclear gluon distribution, especially at small x and large Q^2 region, and nuclear quark distribution at large x for all sets of nPDFs.

In this work, we study the isolated prompt photon and γ +jet productions in proton-lead collisions at LHC energy $\sqrt{s_{NN}} = 8.16$ TeV with a NLO pQCD program JETPHOX [1, 49, 50] with updated proton’s PDFs – CT14 parametrization [41]. The nuclear parton distribution functions (nPDFs) parametrizations (DSSZ, EPPS16, nCTEQ15) are performed at next-to-leading

order accuracy and the nIMParton is based on Leading Order (LO) calculation with parton-parton recombination. These four sets of nPDFs parametrizations have been utilized in obtaining the cross sections of photon and photon associated jet in p+A collisions. We calculate the nuclear modification factors R_{pPb} for isolated photon production as function of transverse momentum p_T^γ and pseudo-rapidity η^γ at both forward and backward rapidity region, the forward-backward asymmetry Y_{pPb}^{asym} for isolated photon production as function of p_T^γ , and the nuclear modification factors R_{pPb} for γ +jet production as function of $\eta_{\gamma\text{Jet}}$ at limited p_T^{avg} intervals. We address the quantification of dominant Bjorken x regions detected under different specific rapidity and transverse momentum ranges.

This paper is organized as follows: in Section 2, we describe our perturbative QCD predictions of prompt photon associated jet inclusive cross section in proton-proton collisions at 8TeV. In Section 3, we discuss the nuclear modification of isolated prompt photon productions at both forward and backward region at 8.16TeV. In Section 4, the cold nuclear matter effects on photon+jet productions are studied at different transverse momentum intervals at 8.16TeV. And we give the summary in the last Section.

2 PHOTON AND PHOTON+JET PRODUCTIONS IN P+P

High- p_T prompt photons mainly arise from two possible mechanisms in hadronic collisions, produced directly in the hard sub-processes referred to as ”direct” photons or fragmented from energetic parton. We consider that the next-to-leading order(NLO) inclusive cross section for the production of prompt photon with transverse momentum p_T^γ is given by the sum of the fragmentation and direct contributions, written as [1, 50],

$$\sigma(p_T^\gamma) = \hat{\sigma}^D(p_T^\gamma; \mu; M; M_F) + \sum_k \int_0^1 \frac{dz}{z} \hat{\sigma}^F(p_T^\gamma/z; \mu; M; M_F) D_k^\gamma(z; M_F) \quad (1)$$

Where μ is the renormalization scale, M is the initial state factorisation scale and M_F is an arbitrary final state fragmentation scale. The contribution $\hat{\sigma}^F$ denotes the partonic cross section for producing a parton convoluted with the PDF of the incoming proton, and D_k^γ is the fragmentation function of a parton k (quarks, anti-quarks and gluon) into a photon. $\hat{\sigma}^D$ includes the partonic cross section for producing a direct photon and the corresponding PDFs. Experimentally, there are also secondary photons originated from hadron decay during the collisions, therefore an isolation cut would be applied for the substantial production of photons. A photon is isolated if the amount of deposited hadronic transverse energy E_T is not more than an specific upper limit

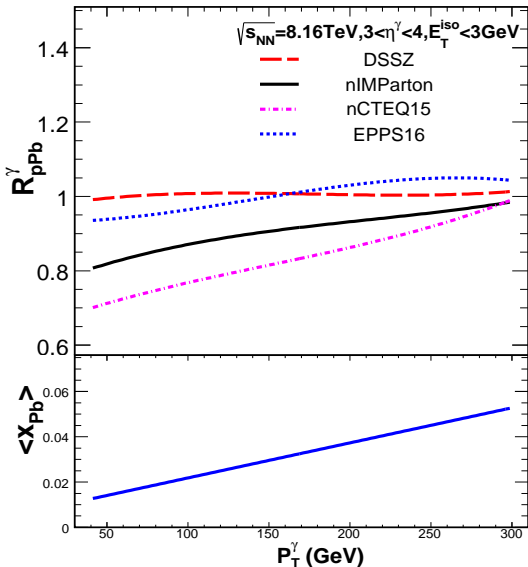


FIG. 2: (Upper) A comparison between the nuclear modification ratios R_{pPb} for p-Pb collisions at $\sqrt{s} = 8.16$ TeV and $3 < \eta^\gamma < 4$ using the nCTEQ15, EPPS16, DSSZ and nIMParton nuclear modifications and the CT14 free-proton PDFs. (Bottom) The corresponding average Bjorken $\langle x_{Pb} \rangle$ as function of p_T^γ .

E_T^{iso} in a fixed radius $R_{\text{iso}} = \sqrt{(\eta - \eta_\gamma)^2 + (\phi - \phi_\gamma)^2}$ in pseudo-rapidity and azimuthal angle around the photon direction. This restriction on the yields of isolated photons could not only reject the secondary decay photons, but also reduce the contribution from fragmentation processes. In the following we focus on the production of isolated photon and isolated photon tagged jets in hadronic collisions.

We calculate isolated photon and jet productions in proton-proton collisions at 8TeV with a next-to-leading order pQCD program JETPHOX [1, 49, 50] with CT14 nucleon parton distribution functions [41] in accordance with the ATLAS experiment [16]. The isolated energy cut for a photon has been set as $E_T^{\text{iso}} < 6\text{GeV}$, and the isolated cone of radius in the pseudo-rapidity and azimuthal angle plane is $R_{\text{cone}} = 0.4$. Moreover photons are selected if its transverse momentum $p_T^\gamma > 130\text{GeV}$ and $|\eta^\gamma| < 2.37$, except $1.37 < |\eta^\gamma| < 1.56$. Jets are reconstructed by anti- k_t algorithm with cone size $R = 0.6$ with $p_T^{\text{jet}} > 100\text{GeV}$ and $|\eta^{\text{jet}}| < 4.4$. In Fig.1, we calculate the differential cross section $d\sigma/dp_T^\gamma$ up to $p_T^\gamma = 1$ TeV in proton-proton collisions at 8 TeV, and our theoretical prediction shows good agreement with the ATLAS experimental results.

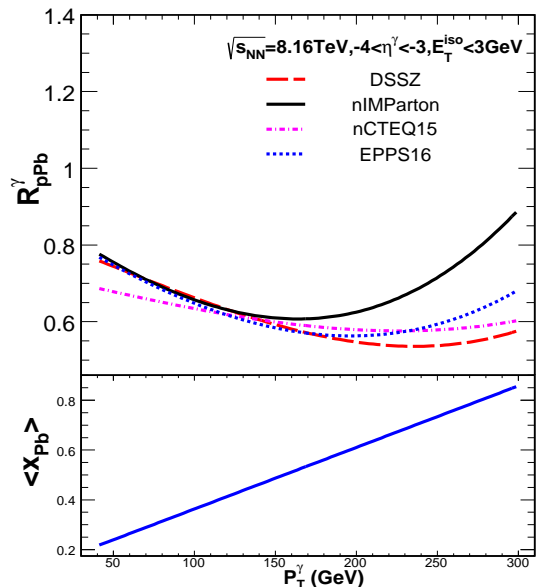


FIG. 3: The same as Fig.2, except at backward rapidity $-4 < \eta^\gamma < -3$.

3 ISOLATED PHOTON IN P+PB COLLISIONS AT VERY FORWARD AND BACKWARD RAPIDITY

The inclusive cross section for the isolated photon production in proton-nucleus collisions could be evaluated by using nuclear PDFs (nPDFs) as substitutes for the free-nucleon PDFs in the collinear factorization framework as stated above, which could effectively include different CNM effects.

In our calculations, we obtain the nPDFs $f_i^A(x, Q^2)$ by multiplying the CT14 parton distribution functions (PDFs)[41] with a flavor and scale dependent factor $R_i^A(x, Q^2)$ taken from four different parametrizations DSSZ [34], EPPS16 [35], nCTEQ15 [42], nIMParton [43]. These four parametrizations for nPDFs are similar that they categorize CNM effects with Bjorken x region into shadowing, anti-shadowing, EMC effect and so on, but differ in the specific formalisms and parameters for describing CNM effects and the input experimental data used in global fits. DSSZ, nCTEQ15, EPPS16 could be convoluted in the expression for calculating the photon production at next-to-leading order(NLO) since they are also quantitated in the NLO pQCD framework. Whereas the leading order results for photon production are applied with nIMParton parametrization to maintain the consistency of the analysis.

The nuclear modification factors in proton+lead collisions are defined as:

$$R_{pPb} = \frac{d\sigma^{pPb}/dp_T}{\langle N_{\text{coll}} \rangle d\sigma^{pp}/dp_T} \quad (2)$$

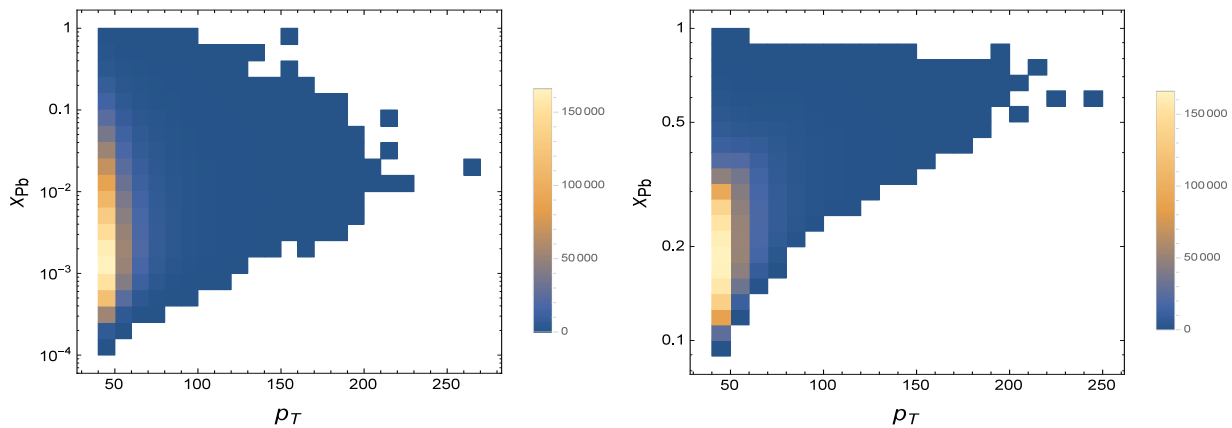


FIG. 4: (Left)NLO fluctuations at Forward rapidity $3 < \eta^\gamma < 4$; (Right)NLO fluctuations at Backward rapidity $-4 < \eta^\gamma < -3$.

with $\langle N_{\text{coll}} \rangle$ representing the number of binary nucleon-nucleon collisions by the glauber model [51].

Now we can make our theoretical predictions for the isolated prompt photon production in p+p and p+Pb collisions at very forward rapidity region $3 < \eta^\gamma < 4$ at $\sqrt{s_{\text{NN}}} = 8.16\text{TeV}$ with ATLAS isolated cuts for photons [16], along with photon's transverse momentum constrained in $40\text{GeV} < p_T^\gamma < 300\text{GeV}$. We display the nuclear modification ratio R_{pPb}^γ as function of p_T^γ in upper panel of Fig.2. And the momentum fraction carried by initial parton from the incoming particle can be roughly estimated at LO as $x_{1,2} = \frac{p_T}{\sqrt{s_{\text{NN}}}}(e^{\pm y_1} + e^{\pm y_2})$, which $x_1(x_p)$ is the initial parton coming from proton on the +z direction, $x_2(x_{\text{Pb}})$ is the initial parton coming from lead on the -z direction in p + Pb collisions and $y_{1,2}$ is the rapidity of γ and the associated jet respectively. The estimated average Bjorken $\langle x_{\text{Pb}} \rangle$ has been defined as the events average value of Bjorken x_{Pb} in JetPhox simulation. In the bottom panel of Fig.2, we show the estimation of the parton's average momentum fraction off nucleus based on NLO results in JETPHOX. We have checked that $\langle x_{\text{Pb}} \rangle$ for nPDFs parametrizations vary slightly from each other, which $\langle x_{\text{Pb}} \rangle$ for nIMParton can be calculated directly at LO. We can see that the average Bjorken $\langle x_{\text{Pb}} \rangle$ is lower than 0.055 at very forward rapidity region, which represents the shadowing effect dominating the CNM effects. Moreover the average Bjorken $\langle x_{\text{Pb}} \rangle$ has a linear positive dependence with p_T^γ expected in its LO estimation.

In the Fig.2, we see that the DSSZ's shadowing effect is unremarkable on the suppression of isolation photon production in p+Pb collisions when the average Bjorken $\langle x_{\text{Pb}} \rangle < 0.055$. We also notice that DSSZ's $R_{\text{pPb}}^\gamma(p_T^\gamma)$ shows a very weak p_T^γ dependence, which means its shadowing effect is nearly independent on photon's transverse momentum in DSSZ at forward rapidity region. Meanwhile the other three parametrizations' shadowing decrease with p_T^γ increasing upon $3 < \eta^\gamma < 4$. Also we can

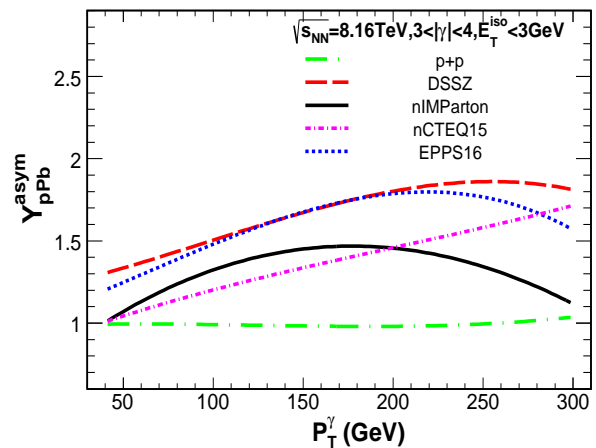


FIG. 5: A comparison between the forward-to-backward asymmetry Y_{asym} for p-Pb collisions at $\sqrt{s_{\text{NN}}} = 8.16\text{TeV}$ and $3 < \eta^\gamma < 4$ using the nCTEQ15, EPPS16, DSSZ and nIMParton nuclear modifications and the CT14 free-proton PDFs.

find that the brand new nPDF parametrization nIMParton's shadowing is only weaker than nCTEQ15's in our discussion.

In Fig.3, similar phenomenon that the positively linear correlation between $\langle x_{\text{Pb}} \rangle$ and p_T^γ has been shown at backward rapidity $-4 < \eta^\gamma < -3$. Whereas the estimated average Bjorken $\langle x_{\text{Pb}} \rangle$ ranges from 0.25 to 0.8, which mostly correspond to EMC effect. We could go a little further to distinguish four different parametrizations' EMC maximum from each nuclear modification factor's extreme point, such as the nIMParton's EMC minimum appears in $p_T^\gamma = 150\text{GeV}$ and the corresponding average Bjorken locates around $\langle x_{\text{Pb}} \rangle = 0.5$, which is the lowest in our results. We further investigate the correlations between x_{Pb} and p_T^γ at both forward and backward rapidities at NLO, shown in Fig. 4. We ob-

serve the broadening of Bjorken x_{Pb} at specific p_T^γ interval due to higher corrections, and the spreading of x_{Pb} at small p_T^γ is rather wider. Also we can see a very dense statistics cluster around the low p_T^γ in our Monte-Carlo simulation, because the possibility distribution of the hard sub-processes for the photon production following double-logarithmic declining with photon's transverse momentum.

Note the nuclear modification factor is sensitive to the nucleon PDF(nPDF) and p+p baseline [52], we may calculate the ratio of the photon production at forward and backward rapidity, which could get rid of the large uncertainty in free nucleon PDFs, which could be used to probe the CNM effects with less arbitrariness[12–14]. We define the forward-backward yield asymmetry as:

$$Y_{pPb}^{\text{asym}} = \frac{d\sigma/dp_T(p + Pb \rightarrow \gamma + X)|_{\eta \in [\eta_1, \eta_2]}}{d\sigma/dp_T(p + Pb \rightarrow \gamma + X)|_{\eta \in [-\eta_2, -\eta_1]}} \quad (3)$$

Our predictions of the forward-to-backward yield asymmetries Y_{pPb}^{asym} for the isolated prompt photon production in p+Pb collisions at $\sqrt{s} = 8.16\text{TeV}$ and $3 < |\eta^\gamma| < 4$ are shown in Fig.5. As a result of the symmetry of the colliding system, there is nearly no forward-to-backward yield asymmetry observed in proton-proton collisions. Y_{pPb}^{asym} is larger than one in p+Pb collisions, which means the photon production suffering more suppression in the backward rapidity region. And the EMC effect reduces the photon production more effectively than the shadowing effect does on the whole. Besides, we notice that the value of Y_{pPb}^{asym} starts going down to one with all parametrizations due to the decreasing of EMC effect at relatively high p_T^γ . This manifestation seems less obvious in nCTEQ15 as its EMC maximum is close to p_T^γ 's highest boundary and our approximate curve fitting.

In order to further explore the impact of input nuclear modifications on the cross section of isolated prompt photon productions in proton-nucleus collision. We further discuss the isolated photon's nuclear modification factor $R_{pPb}^\gamma(\eta^\gamma)$ as a function of photon's rapidity η^γ at both forward and backward rapidities. The Fig.6 tells us that a growing suppression on the photon productions from DSSZ, EPPS16, nIMParton and nCTEQ15 at forward pseudo-rapidity, which quantitatively appears in accordance with the $R_{pPb}^\gamma(p_T^\gamma)$ at $p_T^\gamma = 50\text{GeV}$ due to the highest statistics at lowest p_T^γ region in Monte-Carlo simulations exhibited above in Fig.2. On the other hand, $R_{pPb}^\gamma(\eta^\gamma)$ shows very weak η^γ dependence, because the variation on Bjorken x_{Pb} is at the magnitude of 10^{-3} at region $3 < \eta^\gamma < 4$, shown in the bottom of Fig.6. Combining the results of R_{pPb} evolved with p_T^γ and η^γ , the suppression pattern of isolated photon could be quantitatively analyzed through $\langle x_{Pb} \rangle$ at both forward and backward rapidities. In Fig.7, the nuclear modification factors using four different nPDFs all show the nearly positive linear relation with η^γ , which the val-

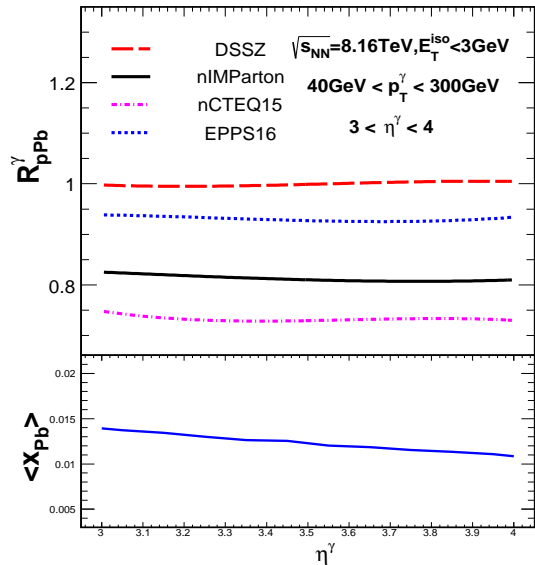


FIG. 6: The same as Fig.2, but as a function of photon's rapidity η^γ .

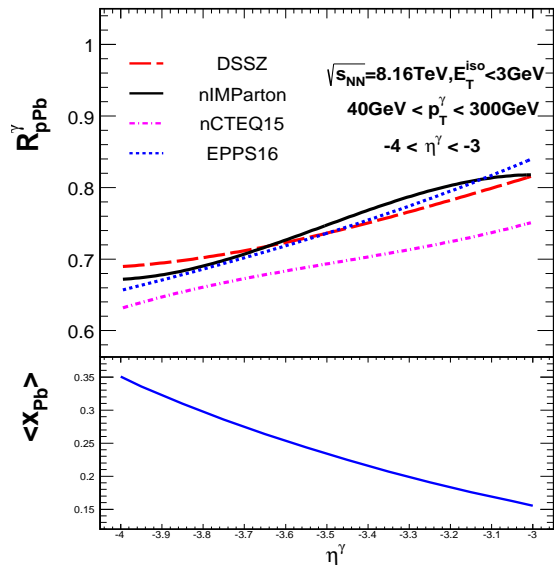


FIG. 7: The same as Fig.3, but as a function of photon's rapidity η^γ .

ues could match with $R_{pPb}^\gamma(p_T^\gamma)$'s through the average Bjorken $\langle x_{Pb} \rangle$, shown in Fig.7 and Fig.3 respectively. And the nCTEQ15 parametrization gives a stronger suppression than the others', which could be confirmed in the prediction of $R_{pPb}^\gamma(p_T^\gamma)$ at low p_T^γ region in Fig.3.

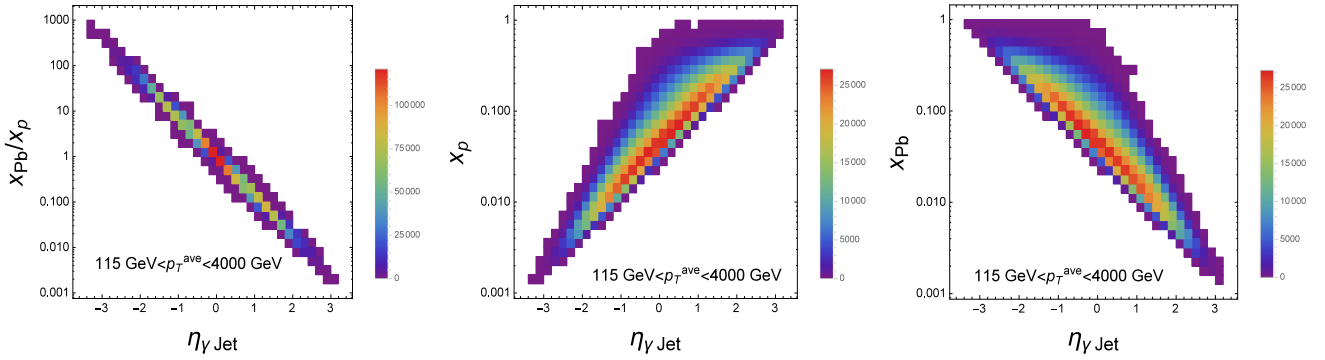


FIG. 8: Correlation between x_{Pb}/x_p (Left), x_p (Middle), x_{Pb} (Right) and γ +jet pseudo-rapidity $\eta_{\gamma jet}$.

4 ISOLATED PHOTON+JET IN P+PB

As compared to isolated photon productions, the isolated photon associated jet production in p+A reactions has more leverage power to access CNM effects in a wider kinematic regions due to its exclusive property. To understand the nuclear modifications for isolated prompt photon associated jet productions, one usually estimates the momentum fractions of the initial-state partons at leading order(LO) to evaluate the CNM effects' contribution by the final-state kinematics, namely $x_{1,2}$ defined above. In the following, we are enlightened by the work on dijets productions in the CMS collaboration [53], and provide the γ +jet pseudo-rapidity $\eta_{\gamma jet} = \frac{1}{2}(\eta_\gamma + \eta_{jet})$ distributions of a photon tagged jet at specific range of their average transverse momentum $p_T^{avg} = \frac{1}{2}(p_T^\gamma + p_T^{jet})$. As $\eta_{\gamma jet}$ would be equal to $\frac{1}{2} \ln(x_p/x_{Pb})$ in the center-of-mass frame when two partons collide with each other at LO. The NLO simulation would give rise to complicated correlations between x_{Pb} (x_p) and $\eta_{\gamma jet}$ describing the nuclear matter's influence, shown in Fig. 8. We also compute the correlations between x_{Pb}/x_p and $\eta_{\gamma Jet}$ at $115\text{GeV} < p_T^{avg} < 4000\text{GeV}$ interval in Fig. 8. It is shown though at NLO accuracy, both distributions of x_{Pb} and x_p over $\eta_{\gamma jet}$ are rather wider, when the ratio x_{Pb}/x_p at NLO is rather narrow and centered at values at LO with very high statistics.

In Fig.9, we can notice that there are tiny shifts on $\frac{\langle x_2 \rangle}{\langle x_1 \rangle}$ as a function of $\eta_{\gamma jet}$ caused by nuclear matter. Based on the relation between $\eta_{\gamma Jet}$ and $\langle x_{Pb} \rangle$, we could reach an assessment about different CNM effects predominate region at $\eta_{\gamma Jet}$, which the γ +jet production is sensitive to shadowing ($\eta_{\gamma Jet} > 1.6$), anti-shadowing ($-0.2 < \eta_{\gamma Jet} < 1.6$), and EMC effects ($\eta_{\gamma Jet} < -0.2$) at $150 < p_T^{avg} < 200$ interval, shown as the black line in Fig.10. The average Bjorken $\langle x_{Pb} \rangle$ shows a nearly negative log-linear relation with $\eta_{\gamma Jet}$, and becomes globally higher when the p_T^{avg} interval increasing.

Furthermore, we discuss the nuclear modification factor for γ +jet production as a function of $\eta_{\gamma jet}$ at $115\text{GeV} < p_T^{avg} < 4000\text{GeV}$ and $200\text{GeV} < p_T^{avg} <$

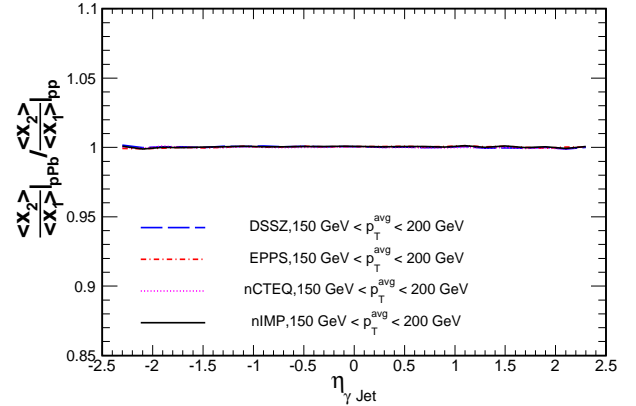


FIG. 9: The ratio of $\langle x_2 \rangle / \langle x_1 \rangle$ in p+Pb and p+p collisions as a function of $\eta_{\gamma jet}$, considering different CNM effects descriptions.

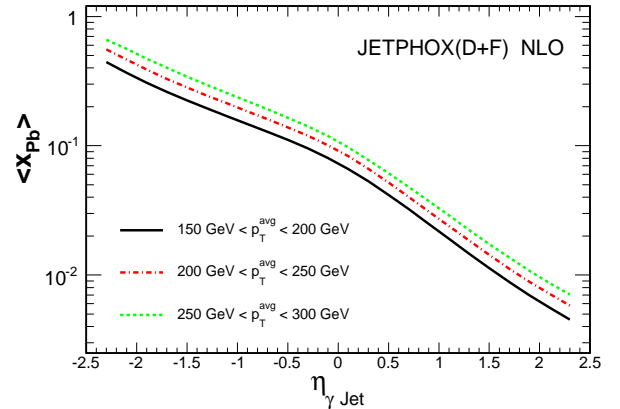


FIG. 10: Mean Bjorken x of the parton from the lead ion x_{Pb} obtained from JetPhox as a function of $\eta_{\gamma jet}$ in different γ +jet events' p_T^{avg} intervals.

250GeV . We have roughly estimated that the nuclear modification factor is sensitive to shadowing when $\eta_{\gamma jet} > 1.6$ and is sensitive to EMC effect when $\eta_{\gamma jet} <$

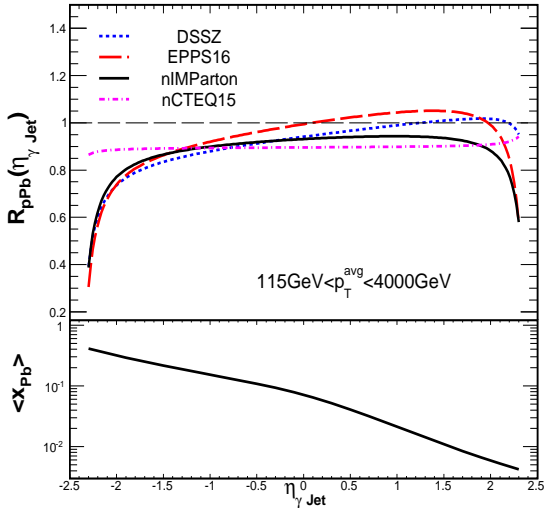


FIG. 11: (Upper) The nuclear modification factor for γ +jet production as a function of $\eta_{\gamma, \text{jet}}$ at $115\text{GeV} < p_{\text{T}}^{\text{avg}} < 4000\text{GeV}$. The NLO pQCD calculation is based on JetPhox with nCTEQ15, EPPS16, DSSZ and nIMParton as the nPDFs. (Bottom) The corresponding average Bjorken $\langle x_{\text{Pb}} \rangle$ as function of $\eta^{\gamma, \text{jet}}$.

-0.2 . In the total average transverse momentum interval ($115\text{GeV} < p_{\text{T}}^{\text{avg}} < 4000\text{GeV}$), we could find that nIMParton offers the strongest shadowing effect, and EPPS16 has the most predominant anti-shadowing effect and EMC effect, along with DSSZ's is in between these two. At the meantime, nCTEQ15 provides a almost constant suppression when $\eta_{\gamma, \text{jet}}$ varies. When the average transverse momentum interval limited to $200\text{GeV} < p_{\text{T}}^{\text{avg}} < 250\text{GeV}$, nCTEQ15's shadowing starts to restore, as well as it remains flattened at small $\eta_{\gamma, \text{jet}}$ and large average Bjorken $\langle x_{\text{Pb}} \rangle$. nIMParton's and EPPS16's shadowing becomes more damped. And EPPS16 has more clear anti-shadowing peak as well as nIMParton and DSSZ begin to reveal anti-shadowing peak. DSSZ provides the strongest EMC suppression at this situation. It is emphasized by leveraging the rapidity and transverse momentum of both photon and jet with measured $p_{\text{T}}^{\text{avg}}$ and $\eta_{\gamma, \text{jet}}$, we can get access to CNM effects in a wide regime and also allocate different kinematics precisely, where differences between varieties of nPDFs sets may be investigated more effectively.

5 SUMMARY

We calculate the productions of isolated prompt photon and γ +jet in p+A with CNM effects from four sets of nuclear parton distribution functions (nPDFs) parametrizations, *i.e.* DSSZ, EPPS16, nCTEQ15, nIMParton, by utilizing the NLO pQCD approach (nIMParton at LO) at LHC 8.16 TeV. We present

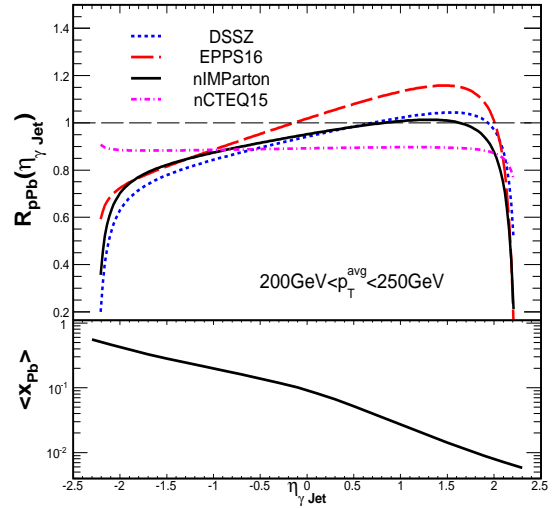


FIG. 12: The same as Fig.11, except for at $200\text{GeV} < p_{\text{T}}^{\text{avg}} < 250\text{GeV}$

the nuclear modification ratio of isolated prompt photon $R_{\text{pA}}^{\gamma}(p_{\text{T}}^{\gamma})$ and $R_{\text{pA}}^{\gamma}(\eta^{\gamma})$, and find shadowing effect and EMC effects dominating at very forward and backward rapidity region respectively. And the rapidity dependence of prompt photon's nuclear modification ratio shows weak rapidity dependence at forward region and varies linearly at backward rapidity region. The production of the isolated photon associated with jet gives us the leveraged power to study the tomography of cold nuclear matter. And the CNM effects of γ +jet productions could be intuitively presented at constraint rapidity $\eta_{\gamma, \text{jet}}$ and average transverse momentum $p_{\text{T}}^{\text{avg}}$ region in our discussion. In terms of sensitivity, comparisons of four different nPDFs parametrizations' cold nuclear matter contribution have been exhibited, and nCTEQ15 shows peculiar results than the others, which could extend our understanding on the constraints of different nPDFs descriptions. It is noted in our work the nPDF parametric form (nIMParton) proposed by Institute of Modern Physics in China has been applied for the first time to investigate hard processes in ultra-relativistic heavy-ion collisions, with a comparison again other three mainstream nPDF groups' predictions.

Acknowledgments: This research is supported by the NSFC of China with Project Nos. 11435004, 11322546, 11805167 and partly supported by China University of Geosciences (Wuhan) (No. 162301182691).

- [1] S. Catani, M. Fontannaz, J. P. Guillet and E. Pilon, JHEP **0205**, 028 (2002) [hep-ph/0204023].
- [2] P. Janus *et al.* [ATLAS Collaboration], KnE Energ. Phys. **3**, 345 (2018).
- [3] P. Ru, B. W. Zhang, L. Cheng, E. Wang and W. N. Zhang, J. Phys. G **42**, no. 8, 085104 (2015)

- [arXiv:1412.2930 [nucl-th]].
- [4] P. Ru, B. W. Zhang, E. Wang and W. N. Zhang, *Eur. Phys. J. C* **75**, no. 9, 426 (2015) [arXiv:1505.08106 [nucl-th]].
- [5] P. Ru and B. W. Zhang, *Nucl. Part. Phys. Proc.* **289-290**, 197 (2017) [arXiv:1612.02899 [nucl-th]].
- [6] P. Ru, S. A. Kulagin, R. Petti and B. W. Zhang, *Phys. Rev. D* **94**, no. 11, 113013 (2016) [arXiv:1608.06835 [nucl-th]].
- [7] S. Chatrchyan *et al.* [CMS Collaboration], *Phys. Lett. B* **710**, 256 (2012) [arXiv:1201.3093 [nucl-ex]].
- [8] X. N. Wang and Z. Huang, *Phys. Rev. C* **55**, 3047 (1997) [hep-ph/9701227].
- [9] X. N. Wang, Z. Huang and I. Sarcevic, *Phys. Rev. Lett.* **77**, 231 (1996) [hep-ph/9605213].
- [10] J. L. Albacete *et al.*, *Nucl. Phys. A* **972**, 18 (2018) [arXiv:1707.09973 [hep-ph]].
- [11] W. Dai, S. Y. Chen, B. W. Zhang and E. K. Wang, *Commun. Theor. Phys.* **59**, 349 (2013).
- [12] I. Helenius, K. J. Eskola and H. Paukkunen, *JHEP* **1409**, 138 (2014) [arXiv:1406.1689 [hep-ph]].
- [13] M. Goharipour and H. Mehraban, *Phys. Rev. D* **95**, no. 5, 054002 (2017) [arXiv:1702.05738 [hep-ph]].
- [14] M. Goharipour and S. Rostami, arXiv:1808.05639 [hep-ph].
- [15] M. Aaboud *et al.* [ATLAS Collaboration], *Phys. Lett. B* **770**, 473 (2017) [arXiv:1701.06882 [hep-ex]].
- [16] M. Aaboud *et al.* [ATLAS Collaboration], *Nucl. Phys. B* **918**, 257 (2017) [arXiv:1611.06586 [hep-ex]].
- [17] The ATLAS collaboration [ATLAS Collaboration], ATLAS-CONF-2017-072.
- [18] A. M. Sirunyan *et al.* [CMS Collaboration], arXiv:1807.00782 [hep-ex].
- [19] A. M. Sirunyan *et al.* [CMS Collaboration], arXiv:1801.04895 [hep-ex].
- [20] A. M. Sirunyan *et al.* [CMS Collaboration], *Phys. Lett. B* **785**, 14 (2018) [arXiv:1711.09738 [nucl-ex]].
- [21] J. C. Collins, D. E. Soper and G. F. Sterman, *Adv. Ser. Direct. High Energy Phys.* **5**, 1 (1989) [hep-ph/0409313].
- [22] R. Brock *et al.* [CTEQ Collaboration],
- [23] Y. L. Dokshitzer, *Sov. Phys. JETP* **46**, 641 (1977) [*Zh. Eksp. Teor. Fiz.* **73**, 1216 (1977)].
- [24] V. N. Gribov and L. N. Lipatov, *Sov. J. Nucl. Phys.* **15**, 438 (1972) [*Yad. Fiz.* **15**, 781 (1972)].
- [25] G. Altarelli and G. Parisi, *Nucl. Phys. B* **126**, 298 (1977).
- [26] D. de Florian and R. Sassot, *Phys. Rev. D* **69**, 074028 (2004) [hep-ph/0311227].
- [27] K. J. Eskola, V. J. Kolhinen and C. A. Salgado, *Eur. Phys. J. C* **9**, 61 (1999) [hep-ph/9807297].
- [28] K. J. Eskola, *Nucl. Phys. A* **910-911**, 163 (2013) [arXiv:1209.1546 [hep-ph]].
- [29] H. Paukkunen, *Nucl. Phys. A* **926**, 24 (2014) [arXiv:1401.2345 [hep-ph]].
- [30] J. Pumplin, D. R. Stump, J. Huston, H. L. Lai, P. M. Nadolsky and W. K. Tung, *JHEP* **0207**, 012 (2002) [hep-ph/0201195].
- [31] J. Gao *et al.*, *Phys. Rev. D* **89**, no. 3, 033009 (2014) [arXiv:1302.6246 [hep-ph]].
- [32] R. D. Ball *et al.* [NNPDF Collaboration], *JHEP* **1504**, 040 (2015) [arXiv:1410.8849 [hep-ph]].
- [33] L. A. Harland-Lang, A. D. Martin, P. Motylinski and R. S. Thorne, *Eur. Phys. J. C* **75**, no. 5, 204 (2015) [arXiv:1412.3989 [hep-ph]].
- [34] D. de Florian, R. Sassot, P. Zurita and M. Stratmann, *Phys. Rev. D* **85**, 074028 (2012) [arXiv:1112.6324 [hep-ph]].
- [35] K. J. Eskola, P. Paakkinen, H. Paukkunen and C. A. Salgado, *Eur. Phys. J. C* **77**, no. 3, 163 (2017) [arXiv:1612.05741 [hep-ph]].
- [36] K. J. Eskola, H. Paukkunen and C. A. Salgado, *JHEP* **0904**, 065 (2009) [arXiv:0902.4154 [hep-ph]].
- [37] S. Chatrchyan *et al.* [CMS Collaboration], *Eur. Phys. J. C* **74**, no. 7, 2951 (2014) [arXiv:1401.4433 [nucl-ex]].
- [38] V. Khachatryan *et al.* [CMS Collaboration], *Phys. Lett. B* **750**, 565 (2015) [arXiv:1503.05825 [nucl-ex]].
- [39] G. Aad *et al.* [ATLAS Collaboration], *Phys. Rev. C* **92**, no. 4, 044915 (2015) [arXiv:1507.06232 [hep-ex]].
- [40] K. Kovarik, T. Jezo, A. Kusina, F. I. Olness, I. Schienbein, T. Stavreva and J. Y. Yu, *PoS DIS* **2013**, 274 (2013) [arXiv:1307.3454 [hep-ph]].
- [41] S. Dulat *et al.*, *EPJ Web Conf.* **120**, 07003 (2016).
- [42] A. Kusina *et al.*, *PoS DIS* **2015**, 041 (2015) [arXiv:1509.01801 [hep-ph]].
- [43] R. Wang, X. Chen and Q. Fu, *Nucl. Phys. B* **920**, 1 (2017) [arXiv:1611.03670 [hep-ph]].
- [44] S. Atashbar Tehrani, *Phys. Rev. C* **86**, 064301 (2012).
- [45] M. Hirai, S. Kumano and T.-H. Nagai, *Phys. Rev. C* **76**, 065207 (2007) [arXiv:0709.3038 [hep-ph]].
- [46] S. Atashbar Tehrani, arXiv:1712.02153 [hep-ph].
- [47] S. A. Kulagin and R. Petti, *Nucl. Phys. A* **765**, 126 (2006) [hep-ph/0412425].
- [48] S. A. Kulagin and R. Petti, *Phys. Rev. C* **90**, no. 4, 045204 (2014) [arXiv:1405.2529 [hep-ph]].
- [49] P. Aurenche, M. Fontannaz, J. P. Guillet, E. Pilon and M. Werlen, *Phys. Rev. D* **73**, 094007 (2006) [hep-ph/0602133].
- [50] Z. Belghobsi, M. Fontannaz, J.-P. Guillet, G. Heinrich, E. Pilon and M. Werlen, *Phys. Rev. D* **79**, 114024 (2009) [arXiv:0903.4834 [hep-ph]].
- [51] D. G. d'Enterria, nucl-ex/0302016.
- [52] CMS Collaboration [CMS Collaboration], CMS-PAS-HIN-12-017.
- [53] A. M. Sirunyan *et al.* [CMS Collaboration], arXiv:1805.04736 [hep-ex].